

Parity Violation in Proton-Proton Scattering at 221 MeV

A. R. Berdoz,¹ J. Birchall,¹ J. B. Bland,¹ J. D. Bowman,² J. R. Campbell,¹ G. H. Coombes,³ C. A. Davis,^{1,3} A. A. Green,¹ P. W. Green,⁴ A. A. Hamian,¹ R. Helmer,³ S. Kadantsev,³ Y. Kuznetsov,^{5,*} L. Lee,¹ C. D. P. Levy,³ R. E. Mischke,² S. A. Page,¹ W. D. Ramsay,¹ S. D. Reitzner,¹ T. Ries,³ G. Roy,¹ A. M. Sekulovich,¹ J. Soukup,⁴ G. M. Stinson,⁴ T.J. Stocki,⁴ V. Sum,¹ N. A. Titov,⁵ W. T. H. van Oers,¹ R. J. Woo,¹ S. Zadorozny,⁵ and A. N. Zelenski⁵

(The TRIUMF E497 Collaboration)

¹*Department of Physics and Astronomy,*

University of Manitoba, Winnipeg, MB, Canada R3T 2N2

²*Physics Division, Los Alamos National Laboratory, Los Alamos, NM 87545, USA*

³*TRIUMF, 4004 Wesbrook Mall, Vancouver, BC, Canada V6T 2A3*

⁴*Centre for Subatomic Research, University of Alberta, Edmonton, AB, Canada T6G 2N5*

⁵*Institute for Nuclear Research, Academy of Sciences of Russia, RU-117334 Moscow, Russia*

(Dated: May 20, 2019)

Abstract

The parity-violating longitudinal analyzing power, A_z , has been measured in $\vec{p}\vec{p}$ elastic scattering at an incident proton energy of 221 MeV. The result obtained is $A_z = (0.84 \pm 0.29(\text{stat.}) \pm 0.17(\text{syst.})) \times 10^{-7}$. This experiment is unique in that it selects a single parity violating transition amplitude ($^3P_2 - ^1D_2$) and consequently directly constrains the weak meson-nucleon coupling constant h_ρ^{pp} . When this result is taken together with the existing $\vec{p}\vec{p}$ parity violation data, the weak meson-nucleon coupling constants h_ρ^{pp} and h_ω^{pp} can, for the first time, both be determined.

PACS numbers: 11.30.Cp, 21.30.Fe, 25.40.Cm

At the fundamental level, the weak interaction between nucleons is due to heavy boson (W^\pm and Z^0) exchanges between quarks. However, at low and intermediate energies a single meson exchange model with one strong, parity conserving, and one weak, parity non-conserving vertex is often used to describe parity violating effects. The parameters of the strong vertex are already quite well measured, while the weak interaction is parameterized by a set of six weak meson-nucleon coupling constants h_π^1 , $h_\rho^{0,1,2}$, and $h_\omega^{0,1}$, where the superscripts indicate the isospin change and the subscripts denote the exchanged meson. These couplings were calculated by Desplanques, Donoghue, and Holstein (DDH) [1] from the Weinberg-Salam model and quark bag wave functions. Subsequent calculations of the weak meson-nucleon coupling constants have been carried out by a number of authors [2, 3, 4, 5, 6], but it is apparent that the constants still carry considerable ranges of uncertainty (see reviews [7, 8]).

The value of the weak meson-nucleon couplings has implications outside nuclear parity violation. For example, Holstein[9] has concluded that a small value of h_π^1 cannot be understood unless the current algebra quark masses are increased by about a factor of two over the original Weinberg values, which tends to produce a similar suppression of theoretical estimates in other processes, e.g., the still questioned $\Delta I = 1/2$ rule for flavour changing weak decays. In addition, more precise values for the weak meson-nucleon couplings would permit better theoretical calculation of the proton anapole moment [10, 11] which, in turn, would improve calculations of the axial vector radiative corrections needed to interpret electron-proton parity violation experiments such as SAMPLE at MIT-Bates, and G-zero at TJNAF.

Experimentally, the most accessible parity violating observable in pp scattering is the longitudinal analyzing power, $A_z = (\sigma^+ - \sigma^-)/(\sigma^+ + \sigma^-)$, where the + and - signs refer to the helicity state (right or left handed) of the longitudinally polarized incident proton beam, and σ is the scattering cross section. This letter reports the result for A_z obtained by experiment 497 at TRIUMF.

A measurement of A_z in p-p scattering is sensitive only to the short range interaction mediated by ρ and ω exchanges; the π^0 is its own antiparticle, so parity violating π^0 exchange would also be CP violating and is therefore suppressed by a factor of about 2×10^{-3} . Further, the TRIUMF 221 MeV measurement is designed to reject the effects of ω exchange. This is achieved by choosing the incident energy so that the contribution to A_z from the ($^1S_0 - ^3P_0$) transition amplitude integrates to zero over the acceptance of the apparatus, leaving the contribution of the ($^3P_2 - ^1D_2$) transition, which arises essentially only from ρ exchange[12]. For example, with the assumptions of Hamian [13], integrating over the detector acceptance gives $h_\rho^{pp} = h_\rho^0 + h_\rho^1 + h_\rho^2/\sqrt{6} = -33.8 A_z^{expt}$. Including the energy dependence of the PNC transition amplitude gives $h_\rho^{pp} = -30.2 A_z^{expt}$. Precise measurements of A_z have already been made at 13.6 MeV [14] and at 45 MeV [15]. However, unlike the present measurement of A_z , which is proportional to h_ρ^{pp} , the low energy results are proportional to a linear combination of h_ρ^{pp} and h_ω^{pp} with $h_\omega^{pp} = h_\omega^0 + h_\omega^1$. By combining the present measurement with the low energy result, h_ρ^{pp} and h_ω^{pp} can be determined individually.

The layout of experiment 497 is shown in Figure 1. A 200 nA proton beam with a longitudinal polarization of 0.75 ± 0.02 is incident on a 0.40 m long liquid hydrogen (LH_2) target. Transverse electric field ion chambers (TRIC1 and TRIC2) located immediately upstream and downstream of the target, measure the change in transmission when the helicity of the incident beam is reversed.

The optically pumped polarized ion source (OPPIS)[16] minimizes unwanted helicity

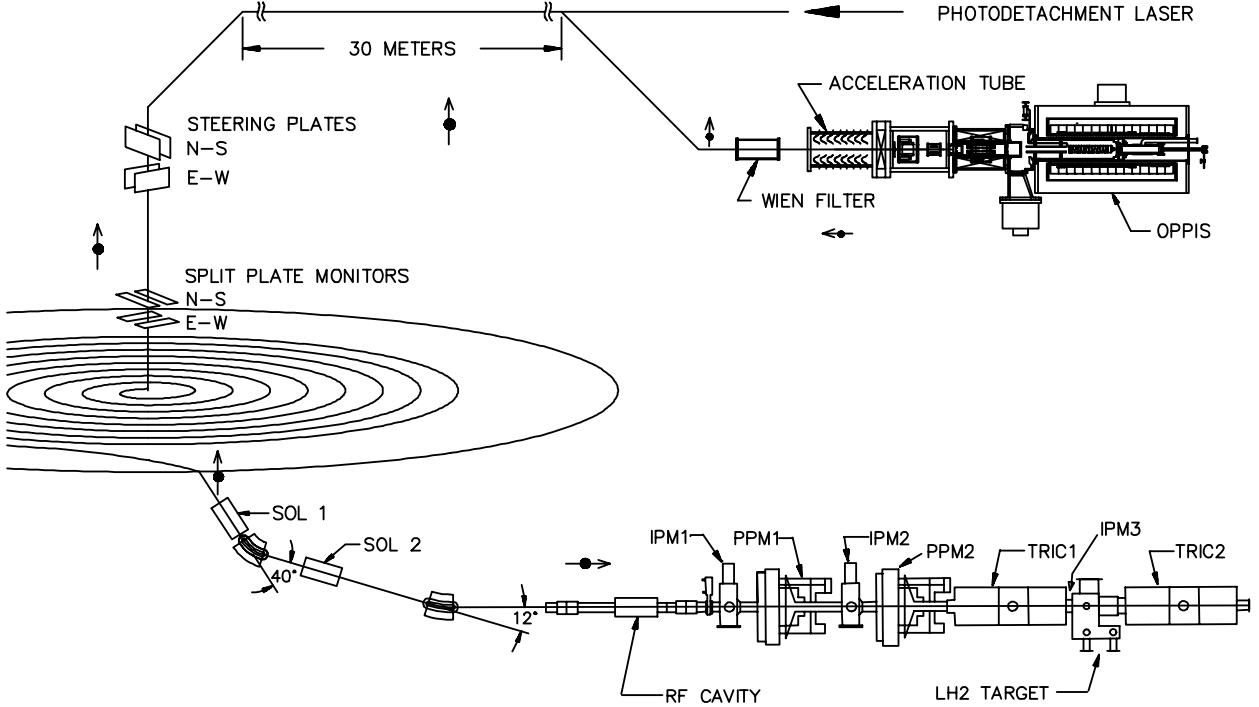


FIG. 1: General layout of the TRIUMF p-p parity violation experiment.(OPPIS: Optically Pumped Polarized Ion Source; SOL: spin precession SOLenoid magnet; IPM: Intensity Profile Monitor; PPM: Polarization Profile Monitor; TRIC: TRansverse electric field Ionization Chamber). One of eight possible spin configurations of ion source, cyclotron and experiment is indicated.

correlated modulations of beam properties. Helicity reversals are implemented at OPPIS by changing the frequency of the lasers which optically pump Rb vapor whose polarization is ultimately transferred to the protons of the H^- beam. No macroscopic electric or magnetic fields are altered. The polarization of the Rb vapor is measured every spin state and is relayed back to the experiment encoded as a frequency to avoid having helicity correlated levels in the electronics racks. By running the full data acquisition system and ion source, with a current source replacing the main ion chambers, cross talk from the helicity signal was shown to be negligible.

After the ion source, a Wien filter orients the spin direction so that it is vertical in the cyclotron. The 221.3 MeV beam is extracted from the cyclotron and a solenoid - dipole, solenoid - dipole magnet sequence rotates the spin to the longitudinal direction. The magnets can be set to rotate spin-up in the cyclotron to either right handed (+) or left handed (-) helicity at the parity apparatus.

In the last section of beam line, the longitudinally polarized beam passes first through a series of diagnostic devices – a set of two beam intensity profile monitors (IPMs)(reference [17] describes an older version) and a pair of transverse polarization profile monitors (PPMs) [18]. A third IPM is located immediately in front of the LH_2 target, inside the cryostat.

The LH_2 target has a flask of 0.10 m diameter and a length of 0.40 m with flat and parallel end windows. Rapid (5 L/s) circulation of the LH_2 reduces the density gradients to an acceptable level.

The TRICs contain field shaping electrodes plus guard rings to ensure a uniform sense region, 0.15 m wide by 0.15 m high by 0.60 m long between the parallel electrodes. The

TRICs are filled with ultra-high purity hydrogen gas and operated at a pressure of about 150 Torr and a high voltage of -8 kV. The entrance and exit windows are located approximately 0.9 m from the center to range out spallation products and thus prevent their entering the active region. False parity violating signals due to the buildup of radioactivity as a result of beam exposure were estimated to be negligible.

The sensitivity to each kind of helicity correlated modulation is measured in separate calibration runs in which each beam parameter (intensity, size, position, transverse polarization) is intentionally modulated at an enhanced level. The sensitivity is then multiplied by the coherent modulation measured during actual data taking and a correction is applied.

Beam position information is derived from the IPM signals, based on secondary emission from thin nickel foil strips placed between thin aluminum foils. The 31 harp signals from each of six planes are individually amplified and digitized to provide the beam intensity profiles in each spin state. The beam centroids at two IPM locations are obtained through integration of the discrete distributions; a corresponding correction signal is used to drive feedback loops to a pair of horizontal and vertical fast, ferrite-cored steering magnets. This position servo holds the beam to within $50\mu\text{m}$ of the “neutral axis” on which the experiment is insensitive to average transverse polarization components. Sensitivities to helicity-correlated position and size modulations are determined with the beam unpolarized and enhanced modulations introduced using fast, ferrite cored magnets synchronized to the spin sequence.

Transverse polarization components are measured by the PPMs, which are based on p-p elastic scattering using CH_2 blade targets that are scanned through the beam at the beginning of each spin state, immediately prior to the TRIC integration interval. Each PPM contains detector assemblies for ‘left’, ‘right’, ‘down’, and ‘up’ scattered protons. The CH_2 blades are 1.6 mm transverse to the incident beam direction and 5.0 mm along the beam direction and move through the beam on a circle of 0.215 m radius with a frequency of 5 revolutions per second. Each PPM has four blades, two which scan the polarization profile in the horizontal direction and two which scan the polarization profile in the vertical direction. By scanning transversely polarized beams horizontally and vertically, the polarization “neutral axis” mentioned above can be found.

To extract A_z , measurements in alternating beam helicity are acquired according to an eight state spin cycle. A switching pattern based on the sequence $(+ - - + - + + -)$ or its complement, is used, canceling both linear and quadratic drifts. Each spin state lasts 25 ms, comprising settling time, time for one polarization scan, and a 16.67 ms (1/60 s) TRIC and IPM integration window. The master clock for sequencing the whole experiment, including helicity changes, is derived from optical encoders mounted on the PPM drive shafts. All eight blades of the two synchronized PPMs pass once through the beam in one 200 ms cycle. The 1/60 s integration time is chosen to reject all noise at 60 Hz and its harmonics. To permit a check to be made for unrejected 60 Hz noise, a small controlled phase slip is introduced so that the master clock drifts through one complete cycle of the 60 Hz line every 18 minutes.

The parity detection apparatus attains minimal sensitivity to beam current modulations by precision analog subtraction of the ionization current signals of the two TRICs. To tune the subtraction for minimum sensitivity to coherent intensity modulation, an artificially enhanced ($\sim 0.1\%$) helicity-correlated current modulation can be introduced. Under real data taking conditions, helicity-correlated current modulation $\Delta I/I = (I^+ - I^-)/(I^+ + I^-)$ does not normally exceed a few parts in 10^5 . Periods of enhanced coherent current modulation are also interleaved with the “real” data so that corrections for $\Delta I/I$ can be

made.

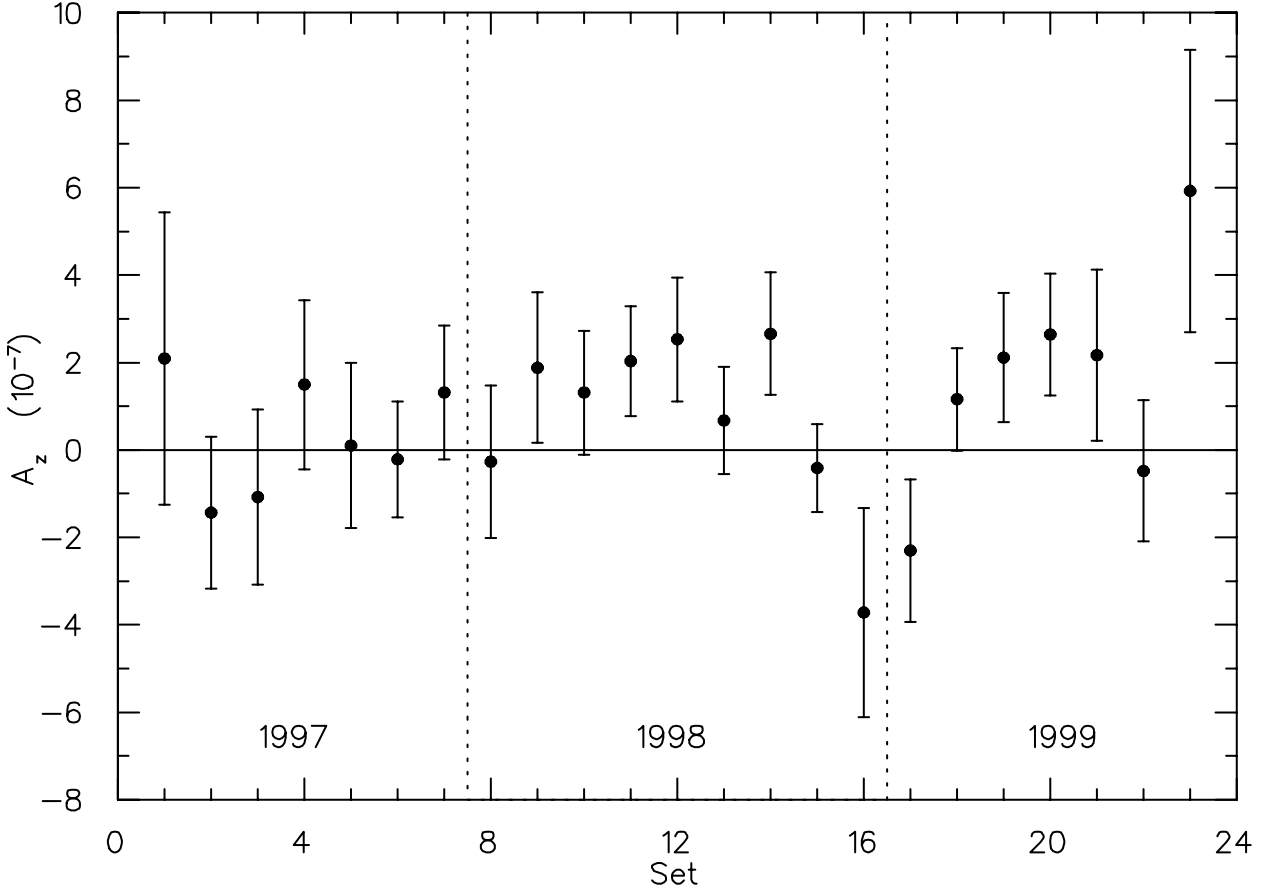


FIG. 2: Corrected A_z data for each of the 23 data sets.

Because the proton energy is on average 27 MeV lower in TRIC2 than in TRIC1, a small change in incident energy changes the signal from TRIC2 more than the signal from TRIC1, and coherent energy modulation appears as a false A_z signal. The sensitivity to coherent energy modulation was determined using a RF accelerating cavity placed upstream of IPM1 in the beam line. The measured sensitivity of $(2.9 \pm 0.3) \times 10^{-8} eV^{-1}$ is in excellent agreement with predictions based on the variation of stopping power with energy. Helicity-correlated extracted energy modulations cannot be directly measured at the parity apparatus, so an appropriate average of data taken with the two beam line helicity tunes is used to minimize the effect on A_z . In addition, interleaved measurements of intrinsic injected energy modulation at OPPIS together with measurements at the parity apparatus of sensitivity to enhanced energy modulation give independent upper limits to the size of the resulting false asymmetries.

The data were taken in three one month-long running periods, divided into 23 sets of alternating beam line helicity. Each data set contains a series of runs, as well as a large number of control measurements, including polarization neutral axis scans, and measurements of the sensitivity to various helicity correlated modulations. Helicity correlated modulations in beam position ($\Delta x, \Delta y$), beam size ($\Delta \sigma_x, \Delta \sigma_y$), beam intensity ($\Delta I/I$), transverse polarization coupled to beam position ($y * P_x, x * P_y$), first moments of transverse polarization ($\langle yP_x \rangle, \langle xP_y \rangle$) and energy modulation at the ion source were considered. Figure 2 shows

TABLE I: Summary of helicity correlated beam properties. The table shows the average value of the coherent modulation, the net correction made for this modulation, and the uncertainty resulting from applying the correction.

Property	Average Value	$10^7 \Delta A_z$
$A_z^{uncorrected}(10^{-7})$	$1.68 \pm 0.29(stat.)$	
$y * P_x(\mu m)$	-0.1 ± 0.0	-0.01 ± 0.01
$x * P_y(\mu m)$	-0.1 ± 0.0	0.01 ± 0.03
$\langle yP_x \rangle(\mu m)$	1.1 ± 0.4	0.11 ± 0.01
$\langle xP_y \rangle(\mu m)$	-2.1 ± 0.4	0.54 ± 0.06
$\Delta I/I(ppm)$	15 ± 1	0.19 ± 0.02
<i>position + size</i>		0 ± 0.10
$\Delta E(meV at OPPIS)$	7–15	0.0 ± 0.12
Total		$0.84 \pm 0.17(syst.)$
$A_z^{corr}(10^{-7})$	$0.84 \pm 0.29(stat.) \pm 0.17(syst.)$	
$\chi^2_\nu(23sets)$	1.08	

the corrected data for the 23 data sets. The uncertainties shown include all contributions except energy modulation. Table I summarizes the helicity correlated beam properties, the net correction made for each, and the uncertainty in each correction. The uncorrected A_z of $(1.68 \pm 0.29) \times 10^{-7}$ becomes $(0.84 \pm 0.29(stat.) \pm 0.17(syst.)) \times 10^{-7}$. The reduced $\chi^2_\nu = 1.08$ shown in Table 1 is derived from the 23 corrected asymmetry values assuming A_z is a constant and that the uncertainties are as shown in Figure 2 (i.e. not including uncertainty in the energy modulation correction). Uncorrected false A_z from energy modulation will have opposite sign in opposite beamline helicities and increase the χ^2_ν . That the χ^2_ν is 1.08 supports the assertion that contributions from uncorrected energy modulation effects are small. An overall systematic uncertainty of ± 0.12 has been assigned for energy modulation.

Note that A_z was measured in a finite geometry with a thick target and requires a further multiplicative correction of 1.02 ± 0.02 when comparing to theoretical predictions at the $(^1S_0 - ^3P_0)$ zero crossing energy (225 MeV) and integrated over all angles. The TRIUMF result (corrected to the $S - P$ zero crossing energy) is shown in Figure 3 together with the most precise results at 13.6 MeV[14] and 45 MeV[15]. Theoretical predictions for A_z from several models [19, 20, 21, 22] are also shown. The model of Driscoll and Miller [19] is based on the Bonn potential to represent the strong N-N interaction together with the weak meson-nucleon coupling constants as given by DDH [1]. The prediction of Iqbal and Niskanen [21] has a Δ isobar contribution added to the Driscoll and Miller model on a semi-ad-hoc basis. The theoretical prediction of Driscoll and Meissner [20] is based on a self-consistent calculation, with both weak and strong vertex functions obtained with a chiral soliton model. Finally, the quark model prediction of Grach and Shmatikov [22] emphasizes the second transition amplitude $(^3P_2 - ^1D_2)$ contribution. None of these predictions are in good agreement with the data, although they all have similar shapes due to the energy dependence of the strong interaction.

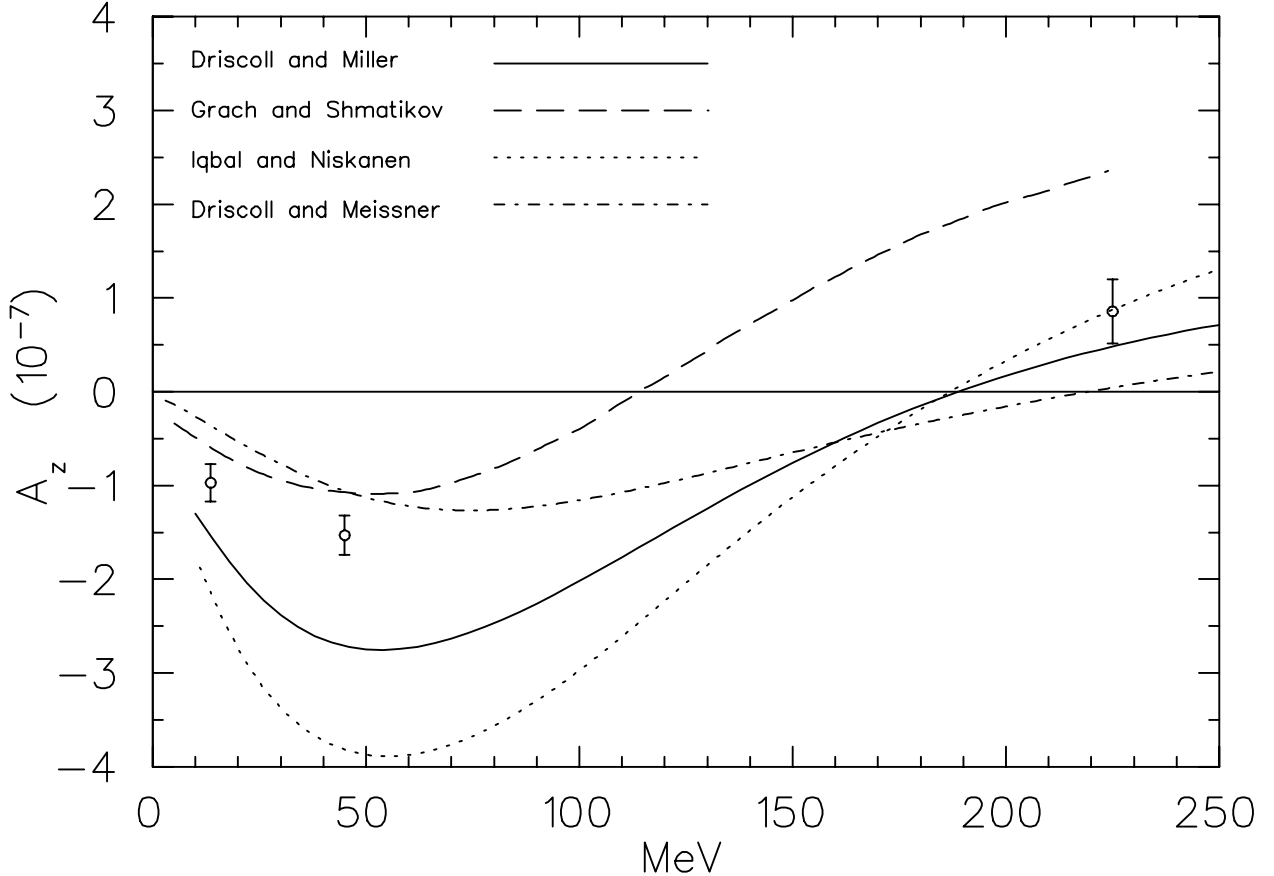


FIG. 3: Theoretical predictions for A_z and the most precise experimental data at 13.6 MeV (Bonn), 45 MeV (SIN) and 221 MeV (TRIUMF).

While the Driscoll and Miller result overestimates the magnitude of A_z at the lower energies by some 50%, it is in agreement with the TRIUMF result at 221 MeV. This confirms that the “best guess value” of DDH for h_ρ^{pp} has about the right size and allows for the first time a delineation of the weak meson-nucleon coupling constants h_ρ^{pp} and h_ω^{pp} using a self consistent formalism connecting these to the measured longitudinal analyzing powers A_z . It can be noted that even though the experimental error of the present experiment is comparable to those at the lower energies, the fractional error and the measure of sensitivity of A_z in terms of h_ρ^{pp} still allows a rather large range of possible values for the latter. A new experiment is being planned at TRIUMF to improve this situation by reducing the error on A_z .

This work was supported in part by the Natural Sciences and Engineering Research Council of Canada; TRIUMF receives federal funding via a contribution agreement through the National Research Council of Canada.

* deceased

- [1] B. Desplanques, J.F. Donoghue, and B.R. Holstein, Ann. Phys.(N.Y.) **124**, 449 (1980).
- [2] V.M. Dubovik and S.V. Zenkin, Ann. Phys.(N.Y.) **172**, 100 (1986).

- [3] G.B. Feldman, G.A. Crawford, J. Dubach, and B.R. Holstein, Phys. Rev. C **43**, 863 (1991).
- [4] N. Kaiser and U-G. Meissner, Nucl. Phys. A **499**, 699 (1989).
- [5] U-G. Meissner and N. Kaiser, Nucl. Phys. A **510**, 759 (1990).
- [6] U-G. Meissner and H. Wiegel, Phys. Lett. B **447**, 1 (1999).
- [7] W.T.H. van Oers, International Journal of Modern Physics E (IJMPE), **8**, 417 (1999).
- [8] W. Haeberli and B.R. Holstein, in *Symmetries and Fundamental Interactions in Nuclei*, edited by W.C. Haxton and E.M. Henley (World Scientific, Singapore, 1995), p. 17.
- [9] B.R. Holstein, in *Proceedings of the Workshop on Spin and Symmetries*, edited by W.D. Ramsay and W.T.H. van Oers, Can. J. Phys. **66**, 510 (1988).
- [10] R. Hasty *et al.*, Science **290**, 2117 (2000).
- [11] W.C. Haxton, C.-P. Liu and M.J. Ramsey-Musolf, Phys. Rev. Lett **86**, 5247 (2001).
- [12] M. Simonius, in *Interaction Studies in Nuclei*, edited by H. Jochim and B. Ziegler, (North Holland, Amsterdam, 1975), p. 3; in *High Energy Physics with Polarized Beams and Targets*, edited by C. Joseph and J. Soffer (Birkhauser Verlag, Basel, 1981), p.355.
- [13] A.A. Hamian, Ph.D.thesis, University of Manitoba (1998), unpublished.
- [14] P.D. Eversheim *et al.*, Phys. Lett. B **256**, 11 (1991); P.D. Eversheim, private communication (1994).
- [15] S. Kistrynn *et al.*, Phys. Rev. Lett. **58**, 1616 (1987).
- [16] C.D.P. Levy *et al.*, in *Proceedings of the International Workshop on Polarized Beams and Polarized Gas Targets* (Cologne, 1995), edited by H.P. gen. Schieck and L. Sydow (World Scientific, Singapore, 1996), p. 120; A.N. Zelenski, *ibid.*, p. 111.
- [17] A.R. Berdoz, *et al.*, Nucl. Instrum. Meth. A **307**, 26 (1991).
- [18] A.R. Berdoz, *et al.*, Nucl. Instrum. Meth. A **457**, 288 (2001).
- [19] D.E. Driscoll and G.A. Miller, Phys. Rev. C **39**, 1951 (1989); *ibid.*, **40**, 2159 (1989).
- [20] D.E. Driscoll and U-G. Meissner, Phys. Rev. C **41**, 1303 (1990).
- [21] M.J. Iqbal and J. Niskanen, Phys. Rev. C **42**, 1872 (1990); private communication (1994).
- [22] I. Grach and M. Shmatikov, Phys. Lett. B **316**, 467 (1993).